LAWRENCE
LIVERMORE
NATIONAL
LABORATORY

LLNL-JRNL-496294

Heating dynamics of CO2-laser irradiated silica particles with evaporative shrinking: measurements and modeling

S. Elhadj, S. R. Qiu, A. M. Monterossa, C. J. Stolz

August 29, 2011

Applied Physics Letters

Disclaimer

Heating dynamics of CO_2-laser irradiated silica particles with evaporative shrinking: measurements and modeling

S. Elhadj[1,a], S. R. Qiu[1], A. M. Monterrosa[2], C. J. Stolz[1]

[1]*Lawrence Livermore National Laboratory, Livermore, CA 94550, USA*
[2]*Department of Nuclear Engineering and Department of Materials Science & Engineering, University of California, Berkeley, CA 94704, USA*

[a]Author to whom correspondence should be addressed. Email: Elhadj2@llnl.gov.

Abstract

The heating dynamics of CO_2-laser heated micron-sized particles were determined for temperatures <3500K measured using infrared imaging. A coupled mass and energy conservation model is derived to predict single particle temperatures and sizes, which were compared to data from particles deposited on non-absorbing substrates to assess the relevant heat transfer processes. Analysis reveals substrate conduction dominates all other heat losses, while laser absorption determined from Mie theory is strongly modulated by particle evaporative shrinking. This study provides insights on the light coupling and heating of particle arrays where the material optical properties are temperature-dependent and particle size changes are significant.

The problem of particle coupling to electromagnetic waves and conversion to thermal energy is involved in a number of fields, including atmospheric sciences,[1] combustion systems,[2] microwave-based food processing,[3] Raman microprobe and laser ablation-ICPM spectroscopy,[4] and laser-assisted particle removal from surfaces.[5] In particular, studies of particle arrays on substrates are receiving increased attention for solar cell energy applications, where packed monolayers of wavelength-scale dielectric spheres are used to enhance light absorption as part of photovoltaic surfaces.[6] Although the field intensification and propagation have been examined,[6,7] issues related to heat generation and dissipation in those arrays have not, and a simple predictive model could prove useful for their design. Here we derive such a model along with temperature measurements on silica spheres exposed to laser irradiation. In the process, we determine the relevant heat and mass transfer mechanisms and the impact of particle shrinking during light coupling. In general, to reduce the influence from nearby particles in the fundamental study of such arrays and to allow interpretation of the data, individual particles need to be isolated. However, isolated particles are difficult to manipulate and suspend when their size is on the order of the wavelength, in addition to the problem of measuring relatively weak and rapidly changing signals.[8]

In this study, micron-sized particle heating dynamics are experimentally addressed by irradiating a monolayer of silica particles on a non-absorbing Germanium substrate with a CW-CO_2 laser under ambient conditions. The assumption is that by restricting the number of neighboring particles to a monolayer their influence is reduced sufficiently that the results can reasonably be interpreted on the basis of a single particle, yet still allow both uniform coupling with the laser and measurements on a well defined extended homogeneous surface. Using *in situ* infrared imaging (described elsewhere[9]) of particle layers deposited by solution-casting from a diluted suspension, the particle heating and cooling was determined during laser exposure from local temperature measurement of the surface (See supplementary **Fig. 1S** of an SEM image of an untreated monolayer, IR image, and temperature spatial profiles). The temporal profiles of the peak temperatures obtained at the center of the heated spot were compared to predicted temperatures based on a simple mass and energy balance using a lumped parameter model given below which, for simplicity, ignores any temperature variations within the particles and assumes homogeneous material properties. A summary of the model parameters is given separately (See **Table IS** in the Supplementary section for description, values, and literature sources).

$$4/3\pi\rho\ C_p da(t)^3 T(t)/dt = \pi a(t)^2 \left[\left(\alpha I_0 Q_{abs}[T(t), a(t)] - k\Delta T(t)/4a(t)\right) - 4\left(\sigma\left(T(t)^4 - T_s{}^4\right) + V_m\left(\Delta H_r + C_p\ \Delta T_0(t)\right) - h_a\ \Delta T_a(t)\right)\right] \qquad \textbf{Eq. 1}$$

$$4/3\pi\rho\ da(t)^3 T(t)/dt = -4\pi a(t)^2 V_m \qquad \textbf{Eq. 2}$$

Briefly, in the coupled **Eq. 1** and **Eq. 2**, *T*(t) and $a(t)$ are the instantaneous temperature and particle radius, respectively. The terms on the right-hand-side represent the laser absorption input, with the following heat losses in order: conduction to the substrate, radiation, evaporation, and free convection to the air. Since the laser wavelength, λ_L=10.6 μm, is close to the 8 μm diameter of the particles used in this study, the laser energy absorption driving the heating of the particles was determined from the Mie scattering solution[10] for a sphere in a non-absorbing medium.[11] The solution

depends on the complex refractive index of the particle material, with the imaginary part, k_e, related to the energy absorption coefficient~$4\pi\ k_e\ /\lambda_L$, where k_e is the temperature-dependent extinction coefficient from the literature[12] (**Fig. 1(A)**) and the real refractive index is taken as constant, $n(\lambda_L)=1.935$.[13] The contribution from the laser light reflected from the substrate to the particle exposure was estimated by calculating the ratio, α~1.5, of the volume-integrated power dissipated~$1/2\omega_L\kappa\boldsymbol{E^2}$ with and without substrate reflection given the dielectric loss, κ, and the laser frequency, ω_L . The electric vector intensities, $\boldsymbol{E^2}$, were obtained from the numerical solution of Maxwell's equation (See Supplementary **Fig. 2S** of the $\boldsymbol{E^2}$ intensity plots and description of the simulations). When exposed to peak experimental intensities approaching 194 kW/cm^2 with a 170 μm Gaussian beam waist (1/e^2), the particles reached temperatures exceeding the silica boiling point (~3000K), and thus their size was reduced during exposure. Typical results from laser irradiation are illustrated in the SEM image in **Fig. 1(B)** showing that both melting and evaporation of the particles have taken place. The vaporization and the resulting particle shrinking, in turn, is expected to affect the particle scattering cross section and temperature. Therefore, to account for that process in the model, the temperature dependent evaporation of silica was determined by measuring the evaporation rate of bulk silica surfaces for a range of CO_2 laser intensities and temperatures as described previously.[14] These measurements and the Arrhenius fitting of the evaporative mass flux, V_m, data are shown in **Fig. 2** with an apparent activation energy of B_m=120.1 kcal/mol. The conduction losses to the Ge substrate were roughly approximated by taking the gradient, ΔT, across ~1/2 particle size. A blackbody approximation was used to estimate the radiative losses, while the free convection was determined from the heat transfer coefficient, h_a.

The calculated particle temperatures for laser power of 4,6,7,8, and 11W are compared directly to data in **Fig. 3(A-E)** where the calculated radii are given by the dashed curves. For all power levels, the model predicts the fast initial rise and the subsequent slower decrease in temperature to within a few 100 K over the five second laser exposure. Aside from the simplifications and approximations noted in the model, there are likely two reasons for the discrepancies. First, the particles do not remain spherical during exposure due to melting, flow, and evaporation (**Fig. 1B**), thus the particles present a flatter contiguous surface with absorption characteristics related to the layer thickness, z, where $Q_{abs}\sim 1-e^{4\pi k_e z/\lambda_L}$. Second, except for the 4W case for which the T<2000 K, the calculated radii shrink by up to ~4 μm, and mostly within the first 200 ms of exposure because of the strong temperature dependence of the evaporation rate. Based on the latter two numbers, the particles would have enough thrust to reach a velocity of ~3 m/s and be expelled from the probed area. Indeed, some of the particles were apparently missing (or pushed on top of others) in the treated area (**Fig. 1B**), which would have affected the IR camera measurements and the apparent temperature. Nevertheless, the model still appears to capture the collective behavior of the heated particle with reasonable accuracy, all the way up to the 11W exposure.

There is a counter-intuitive crossover in the temporal temperature profile (**Figure 3F**), whereby temperatures at the lower laser power eventually become greater than those of particles exposed to higher power levels. This is in contrast to laser heating of bulk silica where no such crossover occurs and temperatures continuously increased over time, while requiring irradiances about two orders of

magnitude lower to reach similar levels.[9] This crossover is also captured by the model in **Fig. 4(A)**. The reason for the crossover becomes apparent when the model calculations are carried out without the mass flux **Eq. 2**, i.e., still accounting for the evaporative heat losses but without allowing for the particle shrinking. This calculation is shown in **Fig. 4(B)**, where the temperatures reach the same peak levels as before but remain there for the duration of the exposure. Therefore, it is the greater reduction in size and absorption cross section (see **Fig. 1(A)**) that occurs for the larger irradiances that limits the subsequent laser energy absorption relative to those at lower irradiances. Taking the 11W (194 kW/cm^2) and 8W (141 kW/cm^2) cases as an example, the end result is a higher final particle temperature at 8W, but greater initial peak temperature at 11W (before evaporation can shrink the particle), hence the observed (**Fig. 3(F)**) and predicted (**Fig. 4(A)**) crossover. Using these two cases, we look more closely at the energy distribution over time **Fig 4(C)**. The bulk of the heat losses occur by conduction to the substrate (> 98%), thus the rest of the heat loss terms such as radiation, convection, and evaporation are not significant. We conclude that it is the laser absorption and its coupling to particle size modulated by evaporation that is significant. In other words, the particles run out of material to absorb and settle at the sub-evaporation temperature of the particle material determined by its final size.

Thus, with the proposed experimental model system, careful temperature measurements, consideration of the particle scattering, and with the experimentally derived evaporation flux of the particle material, this study shows that insights in the mechanisms of laser-particle coupling dynamics can be obtained. A reasonable and simple model is also derived for predicting particle temperatures and radii for cases where particle light absorption is strong, and for which evaporation or size changes are important part of the process.

Acknowledgements

The authors would like to thank Dr. Michael Feit and Dr. Ibo Matthews for useful discussions on silica evaporation chemistry and EM wave/material coupling. This work performed under the auspices of the U.S. Department of Energy by Lawrence Livermore National Laboratory under Contract DE-AC52-07NA27344.

References

[1]A. Macke, J. Mueller, and E. Raschke, J. of the Atmos. Sci. **53**, 2813 (1996).
[2]T. Kolb, W. F. Farmayan, P. M. Walsh et al., Comb. Sci. Tech. **58**, 77 (1988).
[3]K. G. Ayappa, H. T. Davis, E. A. Davis et al., AIChE J. **38**, 1577 (1992).
[4]M. Delhaye, P. Dhamelincourt, and F. Wallart, Toxicol. Environ. Chem. **3**, 73 (1979).
[5]S. D. Allen and K. Imen, Particles of Surfaces 7: Detection, Adhesion and Removal, 253 (2002).
[6]J. Grandidier, D. M. Callahan, J. N. Munday et al., Adv. Mater. **23**, 1272 (2011).
[7]H. A. Atwater, V. E. Ferry, and J. N. Munday, Adv. Mater. **22**, 4794 (2010); M. L. Brongersma, L. Y. Cao, P. Y. Fan et al., Nano Lett. **10**, 439 (2010).
[8]R. E. Spjut, A. F. Sarofim, and J. P. Longwell, Langmuir **1**, 355 (1985).
[9]S. T. Yang, M. J. Matthews, S. Elhadj, V. G. Draggoo, and S. E. Bisson, J. App. Phys. **106**, 103106 (2009).
[10]C.F. Bohren and D.R. Huffman, in *Absorption and scattering of light by small particles* (John Wiley & Sons, New York, 1983), pp. 99.
[11]The particle Mie absorption scattering cross section efficiency was calculated based on the scattering coefficient formalism of Bohren, C.F. and Huffman, D.R. in Ref[10] using Mathematica software (Wolfram Research, Inc., Mathematica, Version 8.0, Champaign, IL (2010)). The code is available upon request.
[12]A. D. McLachlan and F. P. Meyer, Applied Optics **26**, 1728 (1987).
[13]R. Kitamura, L. Pilon, and M. Jonasz, Applied Optics **46**, 8118 (2007).
[14]S. Elhadj, M. J. Matthews, S. T. Yang, D. Cooke, " Evaporation kinetics of laser heated silica in reactive and inert gases based on near-equilibrium dynamics," (submitted).
[15]R. Bruckner, J. Non-Cryst. Solids **5**, 123 (1970).
[16]D. Mann, R. E. Field, and R. Viskanta, WARME STOFFUBERTRAG. -Thermo Fluid Dyn. **27**, 225 (1992).
[17]C. J. Glassbrenner and G. A. Slack, Phys, Rev. A: Gen. Phys. **134**, A1058 (1964).
[18]H. L. Schick, Chem. Rev. **60**, 331 (1960).
[19]S. W. Churchill, Chem. Eng. Commun. **24**, 339 (1983).

FIGURES

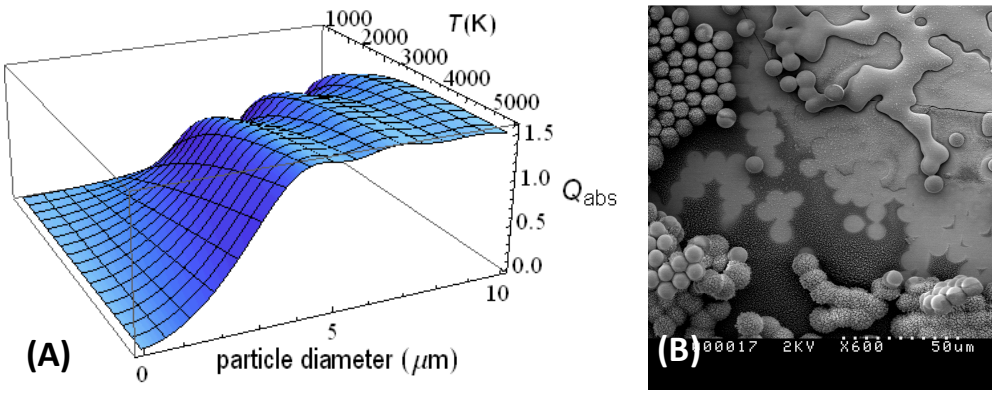

FIG. 1. Calculated Mie absorption scattering efficiency at the laser wavelength of 10.6 μm, Q_{abs} using a temperature-dependent extinction coefficient from Ref[12] for temperatures 300<*T*(K)< 5000 K and particle diameter, $2a$, ranging from 0 to 10 μm (A). The corresponding size parameter, $X=2\pi a/\lambda_L$, range from 0 to 3.0. SEM image of 8 μm diameter silica particles heated with a CO_2 laser beam under ambient air conditions deposited on a non-absorbing Germanium substrate (B). Melted and evaporated particles from CW-CO_2 laser exposed to a Gaussian beam are shown along side unaffected particles. A condensed redeposit silica material appears as a thin "hairy" coating on the particles. Some of the particles appear to have been displaced due to the vaporization thrust, leaving the substrate exposed.

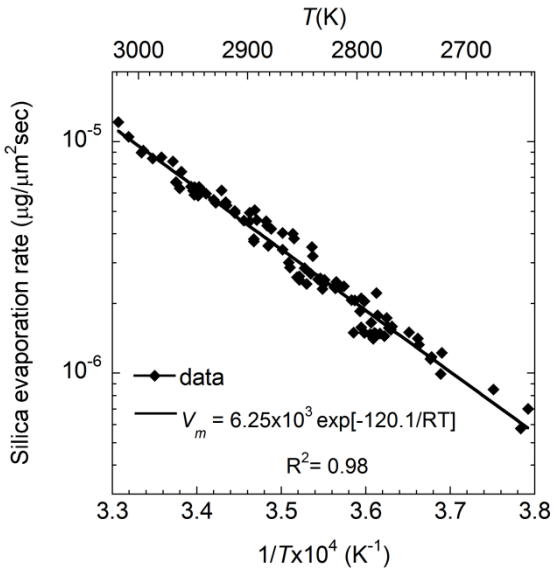

FIG. 2. Measured evaporation rates of bulk fused silica. The temperature dependent evaporation mass fluxes, V_m (mass per area per unit time), were determined using a CO_2 laser for heating in ambient air as described in Ref[14]. The power levels used for heating the surface ranged from 6.5 to 7.2W (880 μm $1/e^2$ beam waist). The rate data were fitted to an Arrhenius expression with an apparent activation energy of 120.1 kcal/mol for the purposes of modeling the particle shrinking rate and the corresponding enthalpy energy dissipated by evaporation given silica evaporation enthalpy from Ref[18].

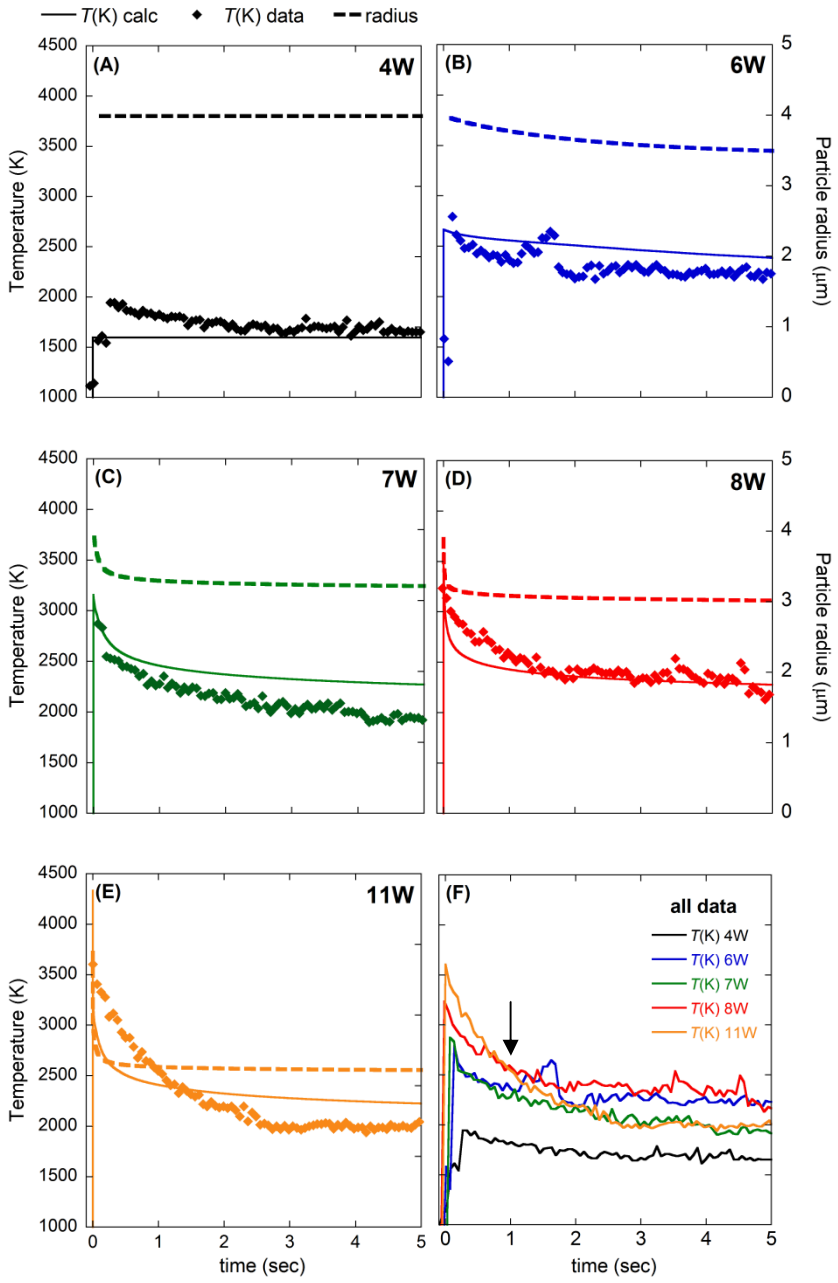

FIG. 3. Experimental temperatures during CO_2 laser exposure of silica particles for the power levels indicated (A-E) were measured by infrared imaging at 16.2 Hz capture rate (Ref[9]). The corresponding calculated temperatures (solid lines) and particle radii (dashed lines) are also shown for each power level. Plot (F) represents all the data curves together from panels (A-E) with the arrow indicating the particle temperature crossover points.

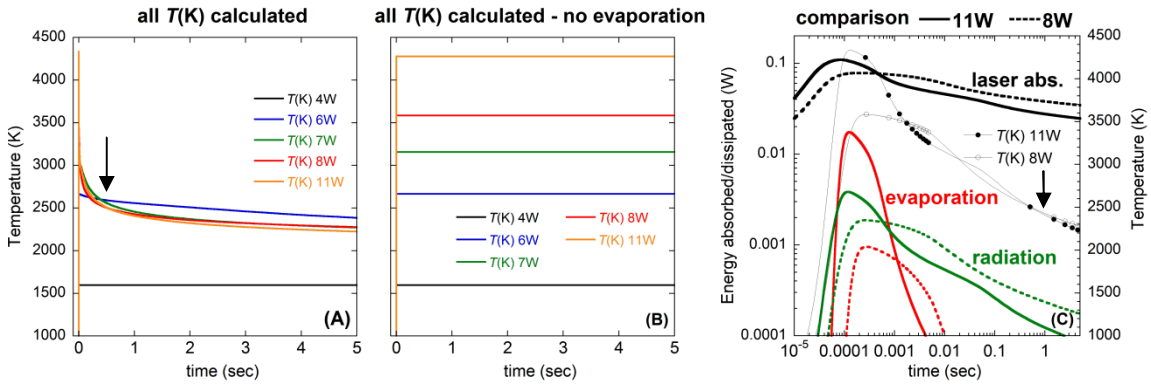

FIG. 4. Calculated temperatures of CO_2 laser heated silica particle during exposure with initial particle diameter of 8 μm with (A) and without (B) evaporative mass losses (but still including evaporative heat losses). 11W (solid lines) and 8W (dashed lines) comparisons of the calculated evolution of the laser energy absorbed and the radiative and evaporative energy dissipated by a particle, with the corresponding temporal temperature profiles (thin lines with points) (C). The balance of the dissipated energy (not shown) is by conduction to the Germanium substrate and tracks the laser energy absorbed represented by the thick solid and dashed black lines. The calculated particle temperatures are also included along with the arrows indicating the temperature crossover points. The energy dissipated by free convection to the air remains well below the other terms in (C) ($<8\times10^{-6}$ W/particle) and thus do not appear in the plot.

SUPPLEMENTARY MATERIAL

Table IS. Description of the model parameters in **Eq. 1** and **Eq. 2** of text given below.

Parameter	Value	Description	Source
ρ	2200 kg/m^3	Silica density	Ref[15]
C_p	1400 J/kg K	Silica specific heat	Ref[16]
α	dimensionless	Ratio of laser power dissipated in particle with and without substrate	calculated
I_0	70 - 194 kW/cm^2	Laser intensity	-
$Q_{abs}(T, a)$	0 - 1.55	Absorption Mie scattering cross section efficiency	calculated
a	8.0 μm (initial)	Particle radius	-
T	300 - ~5000 K	Particle temperature	-
t	0 - 5 sec	Exposure time	-
k	16.9 W/m K	High T Germanium therm conductivity	Ref[17]
ΔT	T - 300 K	T gradient relative to substrate far in the bulk	Calculated
σ	5.67×10^{-8} W/m^2 K^4	Stefan-Boltzmann constant	-
V_m	$A_m$exp[-B_m/RT] μg/μm^2 sec	Silica empirical Arrehnius evaporation flux	This study
T_s	*300 K*	Surrouding radiation T	-
A_m	6.25×10^3 μg/μm^2 sec	Pre-exponential factor	This study
B_m	120.1 kcal/mol	Apparent activation energy	This study
R	1.9859×10^{-3} kcal/mol.K	Gas constant	-
ΔH_r	-7.522×T+194048 cal/mol	Silica evaporation enthalpy	Ref[18]
ΔT_0	300	T increase relative to initial particle temperature	Calculated
h_a	10 W/m^2 K	Free convection in air heat transfer coefficient	Ref[19]
ΔT_a	T - 300 K	T gradient relative to ambient air temperature	Calculated

$$4/3\pi\rho\ C_p da(t)^3 T(t)/dt = \pi a(t)^2 \left[\left(\alpha I_0 Q_{abs}[T(t), a(t)] - k\Delta T(t)/4a(t)\right) - 4\left(\sigma\left(T(t)^4 - T_s{}^4\right) + V_m\left(\Delta H_r + C_p\ \Delta T_0(t)\right) - h_a\ \Delta T_a(t)\right)\right] \quad \textbf{Eq. 1}$$

$$4/3\pi\rho\ da(t)^3 T(t)/dt = -4\pi a(t)^2 V_m \quad \textbf{Eq. 2}$$

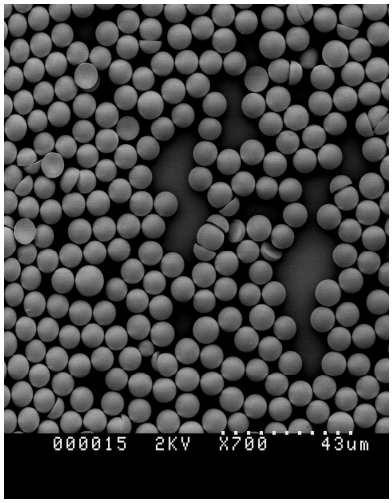

(A)

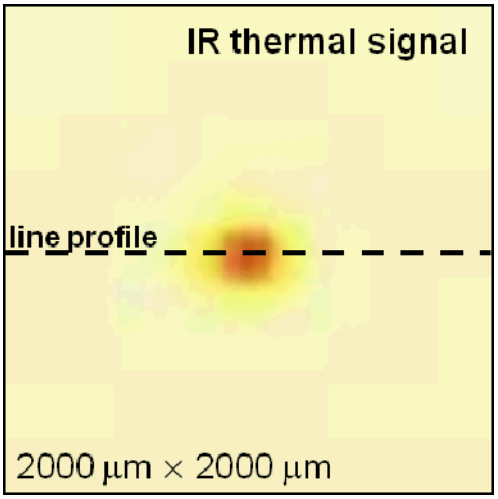

(B)

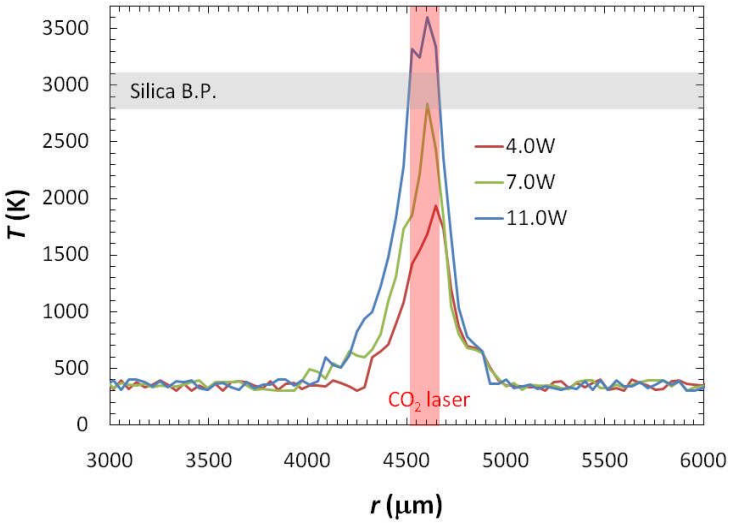

(C)

FIG. 1S. SEM image of a monolayer of fused silica particles obtained by solution casting of a suspension of particles diluted in deionized water (A). The IR thermal image of a monolayer heated with a Gaussian-shaped laser beam (170 μm $1/e^2$ beam waist) was obtained with a LN cooled IR camera at 16.2 Hz with a narrow bandpass cold filter centered at 8.9 ± 0.15 μm and a spatial resolution of ~40μm, as described previously (S. T. Yang, M. J. Matthews, S. Elhadj, V. G. Draggoo, and S. E. Bisson," Thermal transport in CO2 laser irradiated fused silica: In situ measurements and analysis," J. App. Phys. 106 (10), 103106 (2009)) (B). From the IR image, temperature spatial profiles are derived along a line that includes the peak initial temperature reached at the center of the beam, here shown for the cases with laser power of 4, 7, and 11W (C). The 7 and 11W cases reach the silica boiling point (B.P.) as indicated by the grey bar.

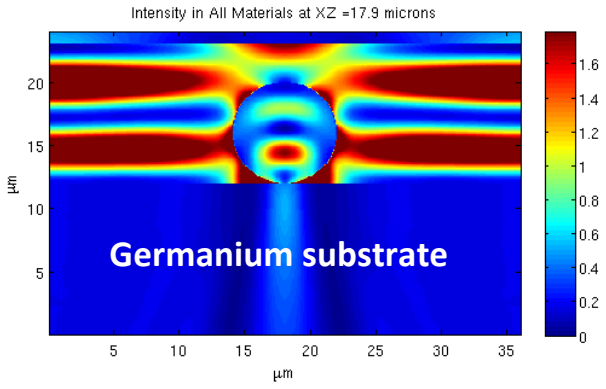

(A)

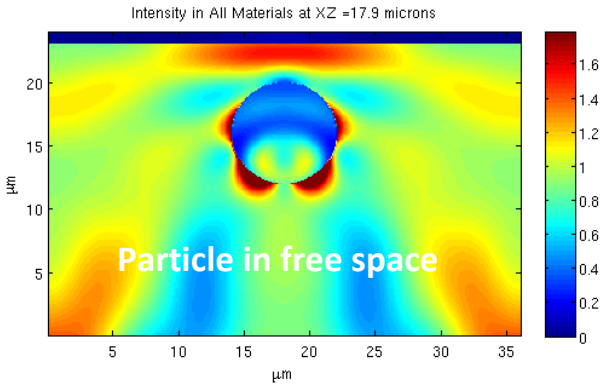

(B)

FIG. 2S. Calculated normalized electric field intensities ($\boldsymbol{E}^2/E_0^2$, E_0=input laser electric field) for a particle on a Germanium substrate (A) and a particle in free space (B) when exposed to P-polarized 10.6 µm laser beam coming from the top of the image down. The narrow solid bar at the top of the image is where the excitation plane begins. A higher color bar scale indicates a higher field enhancement. Simulations were performed using a commercially available code TEMPEST employing a finite-difference time-domain algorithm (FDTD) to solve Maxwell's equations. Detailed description of the FDTD method can be found in the following references: (1) S.R.Qiu, J.E. Wolfe, A.M. Monterrosa, M.D. Feit, T.V. Pistor, C.J. Stolz, "Searching for optimal mitigation geometries for laser-resistant multilayer high-reflector coatings", Applied Optics, 50 (9), C373-C381 (2011), (2) T. Pistor, "Electromagnetic simulation and modeling with applications in lithography," Ph.D. dissertation, University of California at Berkeley, Berkeley, California, (2001), and (3) K. S. Yee, "Numerical solution of initial boundary value problems involving Maxwell's equations in isotropic media," *IEEE Trans. Antennas Propag*. 14, 302–307 (1966).